Development of Fishtail Rudder Sections with Higher Maximum Lift Coefficients

Conference Paper · June 2014

DOI: 10.13140/RG.2.1.3927.7289

2 authors, including:

Trieu Van Nguyen
The University of Danang-University of Science and Technology
34 PUBLICATIONS **121** CITATIONS

SEE PROFILE

Proceedings of the Twenty-fourth (2014) International Ocean and Polar Engineering Conference **www.isope.org**
Busan, Korea, June 15-20, 2014

ISBN 978-1 880653 91-3 (Set); ISSN 1098-6189 (Set)

Development of Fishtail Rudder Sections with Higher Maximum Lift Coefficients

Trieu Van Nguyen, Yoshiho Ikeda
Department of Marine System Engineering, Graduate School of Engineering, Osaka Prefecture University.
Sakai City, Osaka Prefecture, Japan

ABSTRACT

This paper presents theoretical investigations on the performances of several kinds of fishtail rudder sections and hydrodynamic mechanism for generating higher lift forces due to the fish tails. The hydrodynamic forces acting on the sections and the flows passing them are calculated by using a CFD commercial code "Fluent". At first, validation of the computed results is done by comparing the results with experimental results. Secondly, the effect of Reynolds number on the hydrodynamic forces are investigated. Thirdly, hydrodynamic characteristics of several kinds of rudder sections with different shape and fish tails are computed to find the effects of the cross section shapes and the size of fish tail on them.

KEY WORDS: Fishtail; rudder section; high lift, hydrodynamic forces.

INTRODUCTION

For better maneuverability or a smaller rudder of ships, rudders with higher lift and smaller drag have been sought. The ways to increase lift force of lift surfaces were comprehensively introduced in the text books written by Hoerner and Borst (1975) and by A.F. Molland and S.R. Turnock (2007). The books showed that a tail wedge foil, Fig.1a, increases its maximum lift by about 20-30% but is accompanied by higher drag.

Recently, fishtail rudders which have a similar tail shape to the tail-wedge foil are applied for many ships to get higher maneuvering performance due to their higher lift force. The rudders are called Schilling rudder. Maneuverability of pure car carriers (PCC) and VLCCs installed with the Schilling rudder was compared with the same ship installed with normal rudder (Hasegawa, 2004, 2006; Nagarajan, 2008). Their studies showed that Schilling rudder is superior to Mariner rudder not only from the aspect of maneuvering but also from the aspect of fuel efficiency under wind condition.

The hydrodynamic forces acting on the rudder of fish-shape section with end plates were studied by Yuda (2007, 2010a, 2010b) and Kimura (2008).

However, the mechanisms of high lift generation and smaller drag of fishtail rudders still have not been entirely clarified yet. In order to study the mechanisms and the effects of maximum thickness and trailing edge thickness on the lift and drag of fishtail rudders, twelve fishtail sections are designed and named as Fishtail 01~12, and the hydrodynamic forces and flows on/around them are computed in two dimensional flow by CFD in the present study.

RESEARCH BACKGROUND

The fishtail sections are defined as follows:

The maximum width is located at 20% of the chord length (c) from the head, taper to 80%, concave to 90% and flare to 100%.

The profiles of the developed fishtail-rudder sections and NACA0024 are shown in Fig.1b.

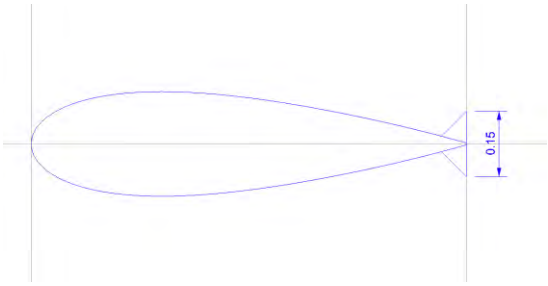

Fig.1a Wedge tail section.

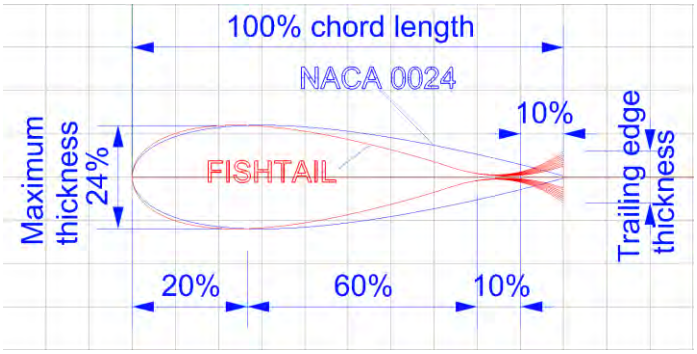

Fig.1b Fishtail-rudder sections and streamlined foil NACA0024.

Twelve fishtail sections can be classified into three groups by maximum thickness (0.24c, 0.18c and 0.12c) and four groups by trailing edge thickness (0.026c, 0.052c, 0.07c and 0.09c) as can be seen in Table 1.

The purpose of these classifications is to reveal the effects of maximum thickness and trailing edge thickness on hydrodynamic forces of fishtail

sections simultaneously.

Table 1 List of Fishtail sections

Name	Maximum Thickness	Trailing Edge Thickness
Fishtail 01	0.24c	0.026c
Fishtail 02		0.05c
Fishtail 03		0.07c
Fishtail 04		0.09c
Fishtail 05	0.18c	0.026c
Fishtail 06		0.05c
Fishtail 07		0.07c
Fishtail 08		0.09c
Fishtail 09	0.12c	0.026c
Fishtail 10		0.05c
Fishtail 11		0.07c
Fishtail 12		0.09c

*where c is the chord length.

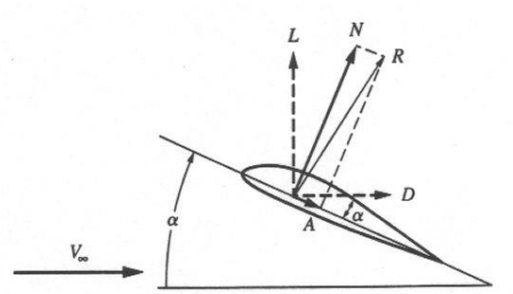

Fig.2 Lift and Drag force directions corresponding to inlet velocity at angle of attack α.

Lift (L) and Drag (D) forces are defined as shown in Fig.2. The lift coefficient C_L is commonly defined by

$$C_L = \frac{L}{\frac{1}{2}\rho v^2 S} \tag{1}$$

where L is the lift force, ρ is fluid density, v is fluid velocity and S is area of the foil (Chord length x Width) .

In the present study, since all calculations by CFD are carried out in the two dimensional condition, the sectional lift coefficient C_l is used for unit span or width. Then the definition of the sectional lift coefficient can be expressed as follow.

$$C_l = \frac{l}{\frac{1}{2}\rho v^2 c} \tag{2}$$

Where l is the lift force acting on two dimensional foil, and c is the chord of the foil.

In the same way, the drag coefficient C_d is defined as:

$$C_d = \frac{D}{\frac{1}{2}\rho v^2 c} \tag{3}$$

where D is the drag force acting on it.

COMPUTATIONAL FLUID DYNAMICS

The lift and drag forces are calculated by using a CFD commercial code, ANSYS FLUENT. The conditions for the calculations are as follows.

The unstructured mesh is automatically generated by using ANSYS Mesh Tool. It would require a very fine mesh near the wall in order to solve for the flow inside boundary layer. The prism layers are applied for the wall boundary. Non-dimensional distance from the wall to the first grid point, y+, is less than 5.

As the turbulent model, the k-omega SST turbulence model is selected. This is a two-equation eddy-viscosity model which has become very popular. The boundary conditions are set as shown in Table 2.

Velocity at inlet is 6 m/s, and the corresponding Reynolds number is 6,000,000.

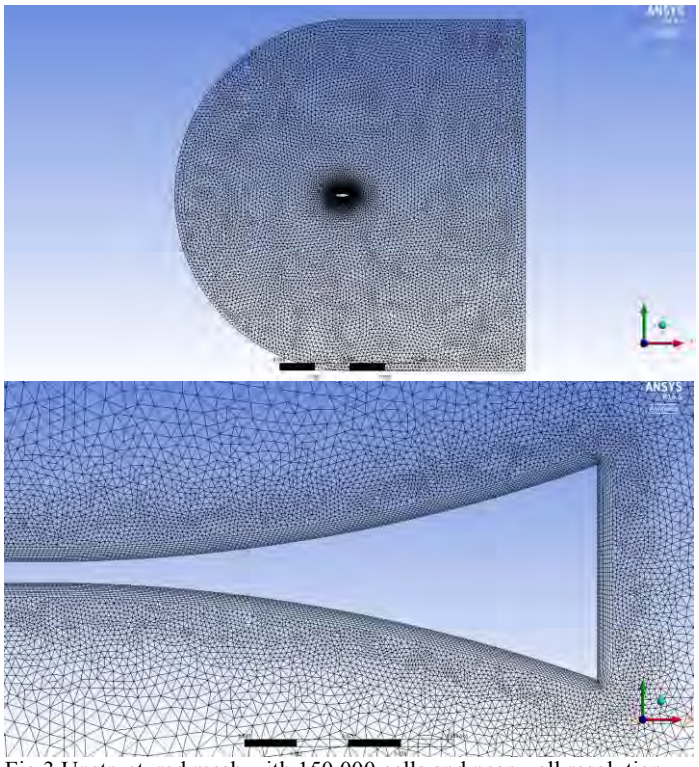

Fig.3 Unstructured mesh with 150,000 cells and near wall resolution.

Table 2 Boundary conditions for CFD calculation

Boundary	Type
Top, Left, Bottom	Velocity inlet
Right	Pressure outlet
Rudder profile	No-slip wall

RESULTS AND DISCUSSIONS

Validations

Before calculating the fishtail rudders, validations of the CFD calculations are carried out. NACA0012 is selected as the cross section for the validation and the calculated results are compared with the experimental and computed data shown by Ladson (Ladson, 1988), CFL3D (NASA LaRC) and Gregory (Gregory, 1970).

Figs.4&5 show the comparisons of the lift and drag coefficients with other data. As shown in Fig.4, the calculated result of the lift shows a good agreement with Ladson and CFL3D data up to stall angle and can give an accurate maximum lift. However, after stall the calculated lift coefficient is higher than that of Ladson's experimental data. This is consistent with the conclusion by Douvi (2012) and may be caused by the turbulent model, k-omega SST model, in the present computations.

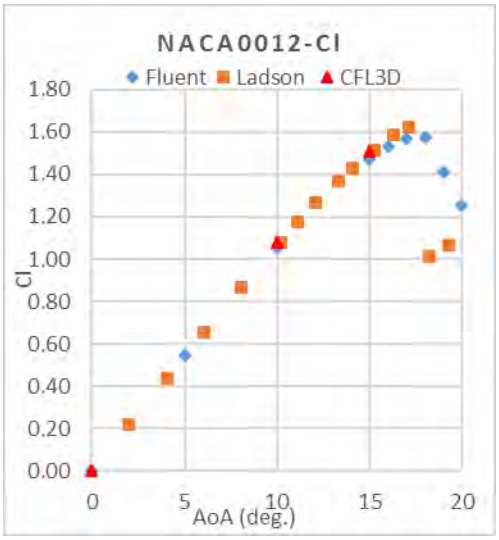

Fig.4 Comparison of the present CFD results and other data for lift coefficients of NACA0012 (AoA: angle of attack)

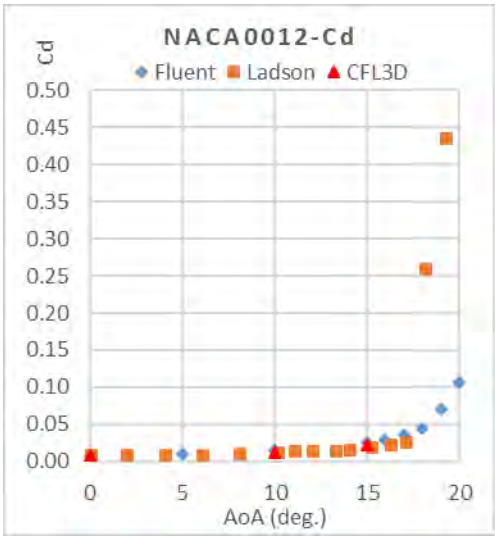

Fig.5 Comparison of the present CFD results and other data for drag coefficients of NACA0012

The calculated drag is also in good agreement with other data up to stall angle as shown in Fig.5.

The present validation demonstrates that the present CFD calculations give us accurate lift and drag in the region of angle of attack below stall angle of the foil.

Fig.6 shows the comparison of pressure coefficients on face and back surfaces of NACA0012 foil between the present CFD results and Gregory data at 15 deg. of angle of attack. The agreement of them is fairly good.

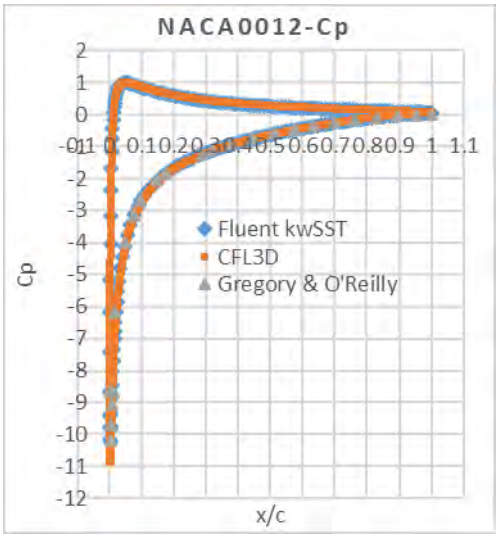

Fig.6 Longitudinal distribution of pressure coefficient on face and back surface of NACA0012 at 15deg of angle of attack

The calculated results of skin friction are shown in Fig.7 with other calculated results, CFL3D. The agreement is fairly good except both ends of the fail, leading and tail ends. This fact suggests that the present calculations can accurately calculate the boundary layer around the foil.

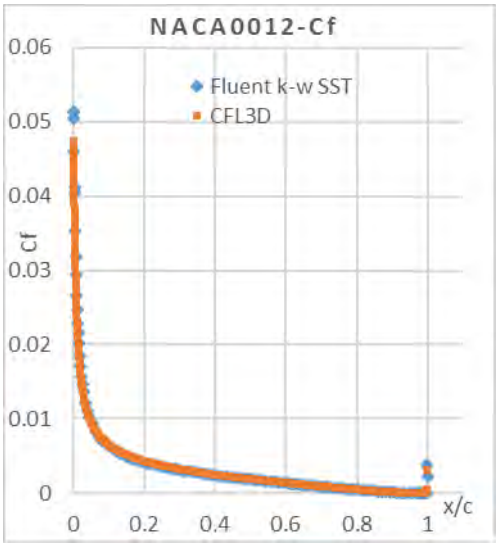

Fig.7 Longitudinal distribution of calculated skin friction coefficient on surface of NACA0012 at 15deg of angle of attack

Effect of Reynolds Number

In this section, the effects of Reynolds number on lift and drag forces acting on a fishtail foil, Fishtail 05, are presented.

Fig.8 shows the lift coefficients of Fishtail 05 at different Reynolds number. Increasing Reynolds number would increase maximum lift coefficient and also delay stall angle. At high Reynolds number over 6 million, increasing of Reynolds number does not effect on the lift coefficient so much and the lift coefficient curves of Fishtail 05 at different Reynolds number have similar characteristic.

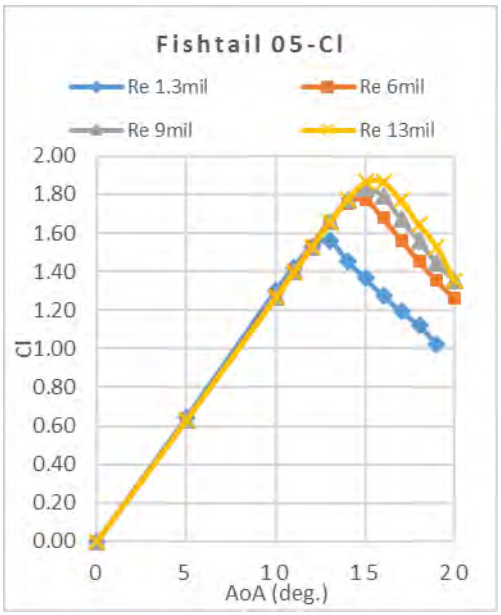

Fig.8 Effect of Reynolds number on lift coefficients of Fishtail 05

Fig.9 shows that Fishtail 05 at low Reynolds number generates larger drag coefficient than that at high Reynolds number. At high Reynolds number the drag coefficients are not significantly influenced by Reynolds number.

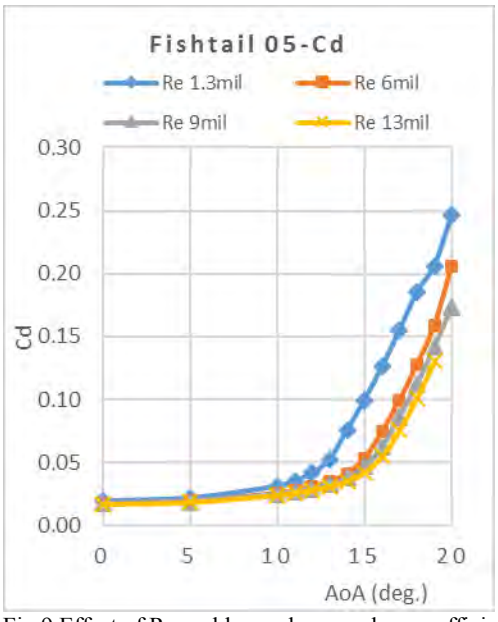

Fig.9 Effect of Reynolds numbers on drag coefficients of Fishtail 05

The effects of Reynolds number on lift to drag force ratio are shown in Fig.10. At higher Reynolds number, Fishtail 05 gives higher maximum lift to drag ratio and in vice versa. From Reynolds number of 6million, the lift to drag curves of Fishtail 05 even at higher Reynolds number have the similar characteristic.

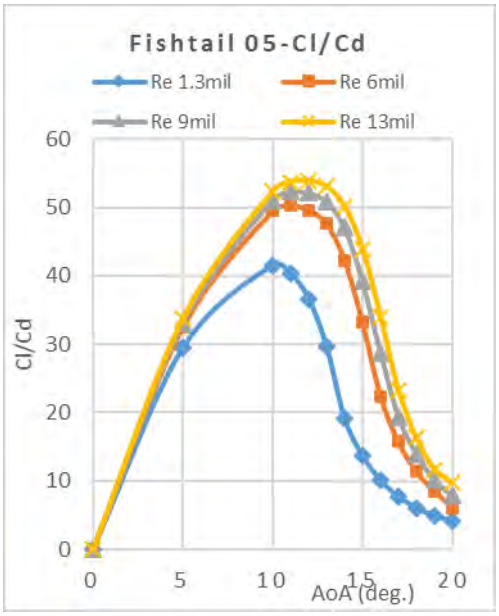

Fig.10 Effect of Reynolds number on lift to drag ratio of Fishtail 05

Basically, at Reynolds number higher than 6million, lift and drag coefficients are not significantly influenced by Reynolds number. Therefore, the Reynolds number of 6million will be selected for further calculations in this study.

Effect of Trailing Edge Thickness

In order to find the appropriate size of the tail, effects of trailing edge thickness on hydrodynamic forces of fishtail sections are investigated.

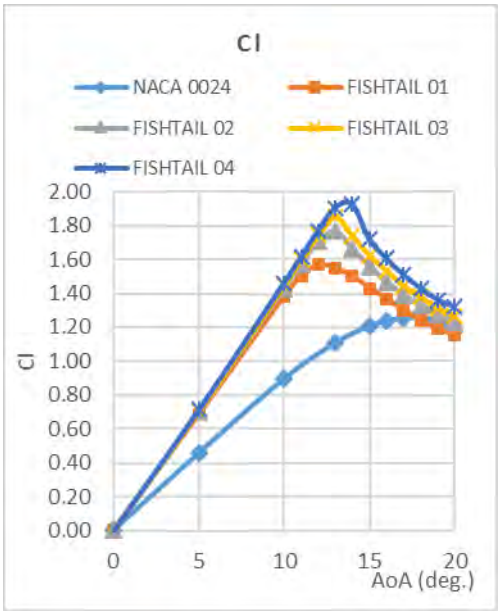

Fig.11 Lift coefficients of Fishtail 01~04 and NACA 0024

The lift coefficients of Fishtail 01~04 are shown in Fig.11. At small angle of attack below 5 deg., all Fishtails give the same lift force but larger lift than NACA0024 which has no fishtail. As increasing the trailing edge thickness, the maximum lift proportionally increases with the thickness of trailing edge. The maximum lift coefficient of Fishtail 04 with the largest trailing edge thickness is highest among them.

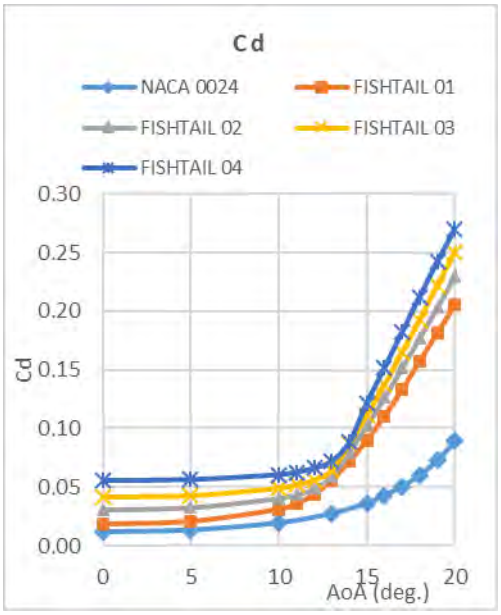

Fig.12 Drag coefficients of Fishtail 01~04 and NACA 0024

Although fishtails increase the lift coefficients, they increase the drag coefficients too, as can be seen in Fig.12. As increasing the trailing edge thickness, the drag increases drastically. For a rudder of a ship, higher lift and lower drag are desirable. Particularly lower drag at small angle of attack is important to reduce the resistance acting a ship.

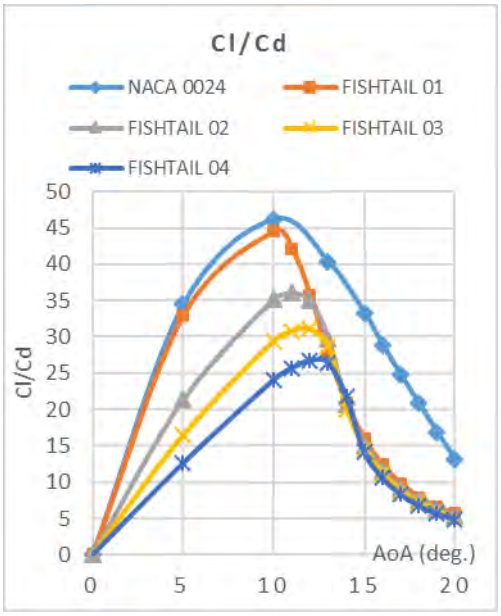

Fig.13 Lift to drag ratio at maximum thickness 24% chord

Fig.13 shows the lift to drag ratio of the foils. We can find that the ratio of Fishtail 01 with the smallest trailing edge thickness is almost same as that of the streamlined NACA0024 in the region of angle of attack below the stall angle. Fig.11 shows that the lift of Fishtail 01 is larger in small angle of attack as other fishtail foils, and its maximum lift is larger than that of the streamlined foil at smaller angle of attack. We can safely say that Fishtail 01 is better than the streamlined foil with the same maximum thickness (24%c) as a rudder of a ship.

To understand hydrodynamic mechanism for higher lift generation and increase of drag of a fishtail, some examples of flow field visualizations around Fishtails 01~04 will be shown in Figs.14~17, pressure and velocity distributions, velocity vectors and stream lines, respectively. In the calculation, angle of attack is kept to be 15 deg.

In the results of pressure distributions shown in Fig.14, we can see that higher pressures are located at two parts on the face side: front one is near the leading edge, while the other is at the concave of rear part near fishtail. The increasing of lift can be explained by the high pressure which covers the concave of the face side.

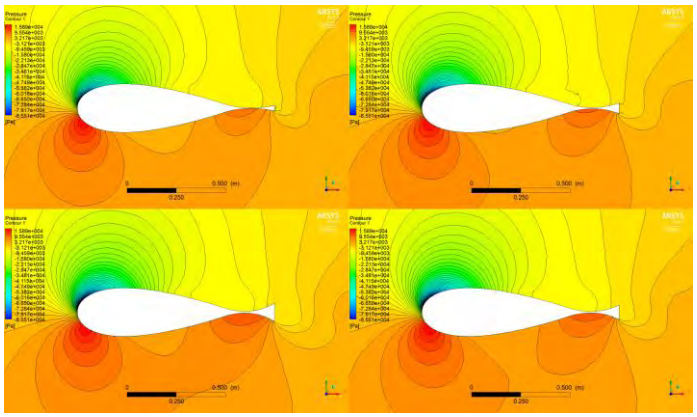

Fig.14 Pressure distribution around Fishtails 01~04 (maximum thickness 24% c) at angle of attack of 13deg.
Top: Fishtail 01 (L), 02 (R); Bottom: Fishtail 03 (R), 04 (L).

Velocity fields shown in Figs.15~17 show that a dead water covers the concave of back (suction) side. It seems that increase of the drag is controlled by the dead water. The dead water in face side disappears with increase of angle of attack, and water flows along the surface in the concave of face side. This flow creates high pressure to increase the lift force.

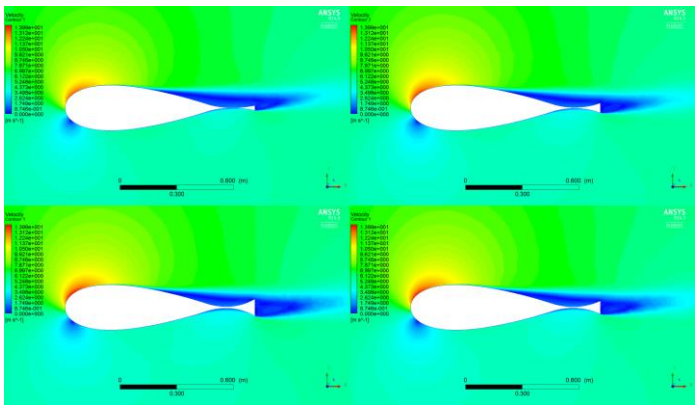

Fig.15 Velocity distribution around Fishtails 01~04 (maximum thickness is 24% c) at angle of attack of 13deg.
Top: Fishtail 01 (L), 02 (R); Bottom: Fishtail 03 (R), 04 (L).

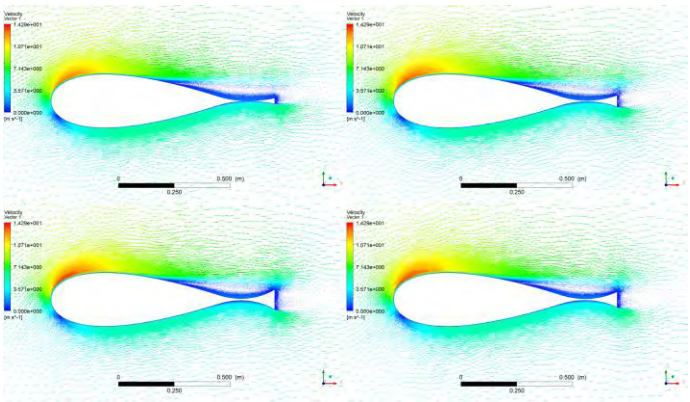

Fig.16 Velocity vectors around Fishtails 01~04 (maximum thickness is 24% c) at angle of attack of 13deg.
Top: Fishtail 01 (L), 02 (R); Bottom: Fishtail 03 (R), 04 (L).

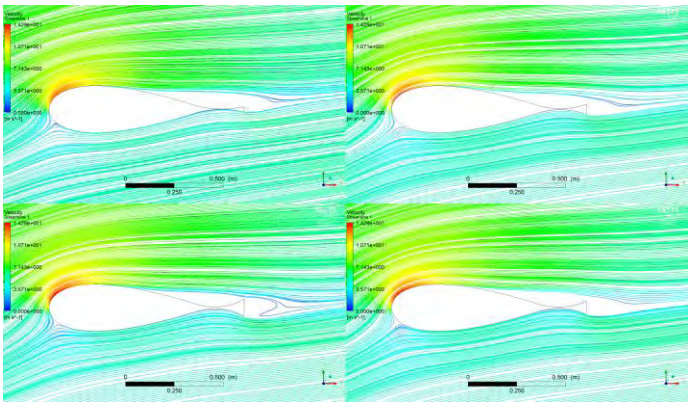

Fig.17 Streamlines around Fishtails 01~04 (maximum thickness is 24% c) at angle of attack of 13deg.
Top: Fishtail 01 (L), 02 (R); Bottom: Fishtail 04 (L), 03 (R).

Discussions and Suggestions

The lift and drag of fishtail foils are controlled by the size of trailing edge. The larger trailing edge gives higher maximum lift but also increases drag significantly and reduces the lift to drag ratio. While the smaller trailing edge increases maximum lift as well as lift at small angle of attack but does not increase the drag, and keeps the lift to drag ratio as almost same as that of the streamlined foil, NACA 0024, up to stall angle.

The calculated results shown in this section demonstrate that a fishtail rudder with small trailing edge has better performance than a conventional streamlined rudder.

Effect of Maximum Thickness

In this section, effects of maximum thickness of fishtail foils are theoretically investigated.

Fig.18 shows the lift coefficient of Fishtails with trailing edge thickness at 0.026% chord which is the same as Fishtail 01 but with different maximum thicknesses. At small angle of attack below 12 deg., the thicker fishtail gives higher lift. However, thinner fishtail delays the stall and gives higher maximum lift. The maximum lift coefficient of the thinnest fishtail foil, Fishtail 09, reaches to 1.8 as shown in Fig.18.

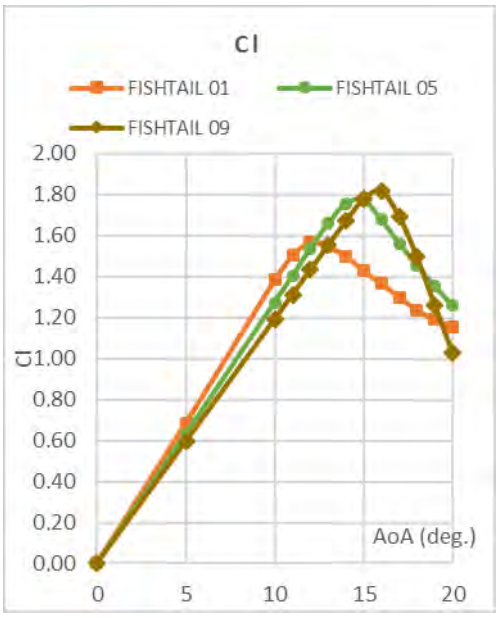

Fig.18 Lift coefficients of Fishtails with different maximum thickness and the same trailing edge thickness as Fishtail 01 (0.026% c)

Fig.19 shows the drag coefficient of Fishtails with different maximum thickness. At small angle of attack below 10 deg., maximum thickness of foils does not effect on the drag coefficient. At higher angle of attack over 10 deg., as foil shape is thicker, the drag coefficients increases.

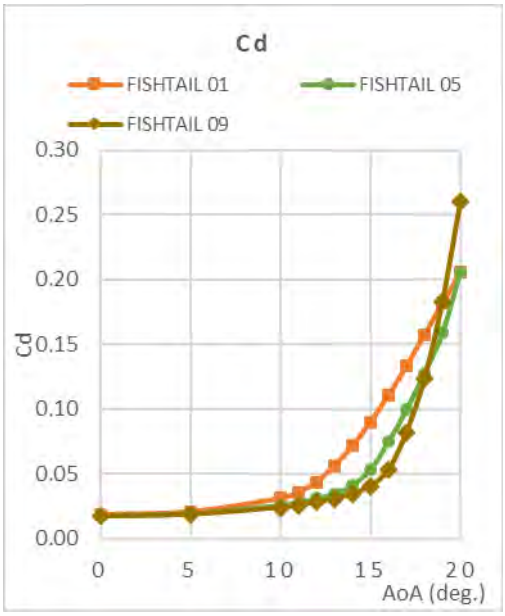

Fig.19 Drag coefficient of Fishtails with different maximum thickness

The effects of maximum thickness on the lift to drag ratio of Fishtails 01, 05 and 09 are shown in Fig.20. At small angle of attack below 5deg., the maximum thickness does not influence the lift to drag ratio. As increasing maximum thickness of foils, however, the maximum lift to drag ratio decreases. The results demonstrate that thinner foil with small fishtail has better performance as a ship rudder.

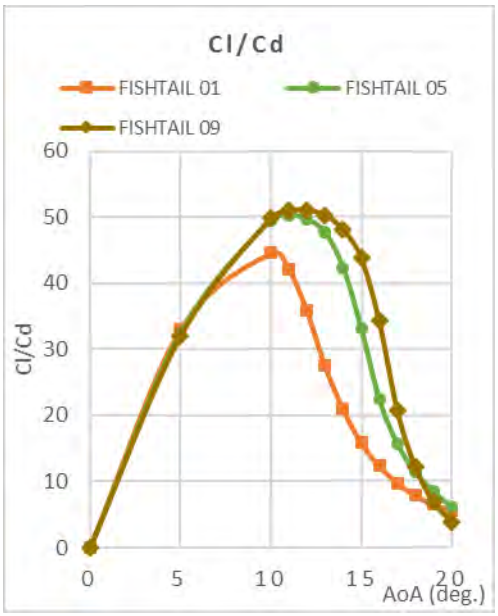

Fig.20 Lift to drag ratio of fishtail foils with different maximum thickness

Pressure and velocity distributions, velocity vectors and stream lines around Fishtails 01, 05 and 09 at angle of attack of 10 deg. are shown in Figs. 21, 22, 23 and 24, respectively.

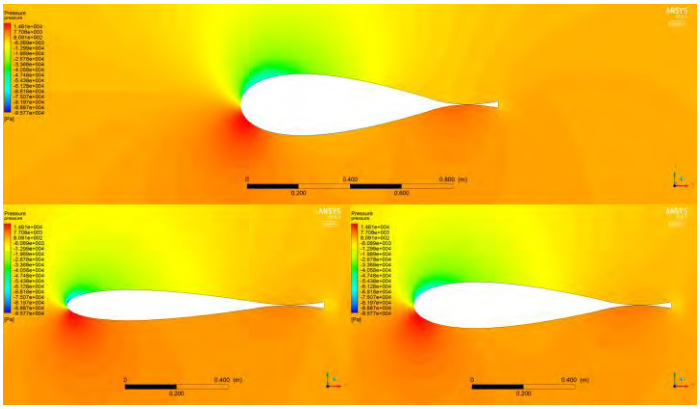
Fig.21 Pressure distribution around Fishtails 01, 05 and 09 at angle of attack of 10deg;
Top: Fishtail 01; Bottom: Fishtail 05 (R), Fishtail 09 (L).

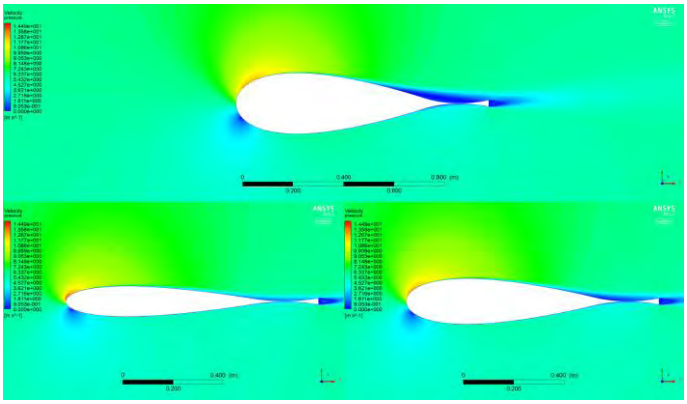
Fig.22 Velocity distribution around Fishtails 01, 05 and 09 at AoA of 10deg; Top: Fishtail 01; Bottom: Fishtail 05 (R), Fishtail 09 (L)

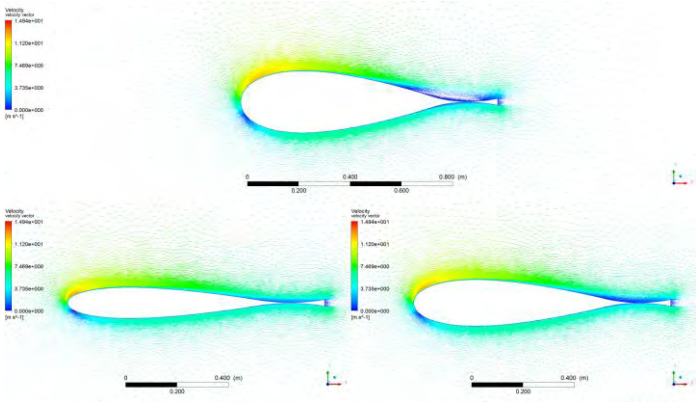
Fig.23 Velocity vectors around Fishtails 01, 05 and 09 at angle of attack of 10deg.
Top: Fishtail 01; Bottom: Fishtail 05 (R), Fishtail 09 (L).

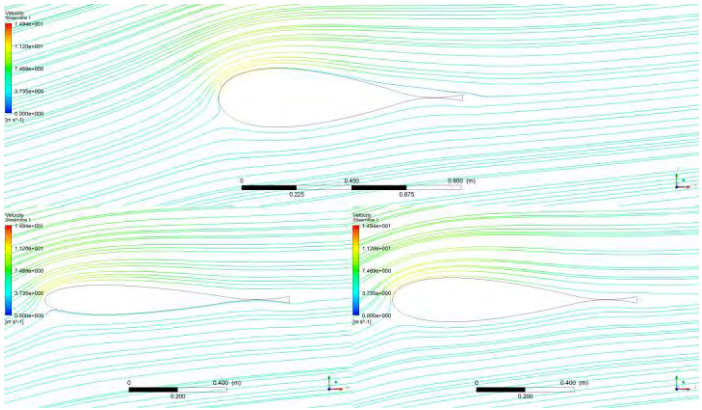
Fig.24 Streamlines around Fishtails 01, 05 and 09 at angle of attack of 10deg.
Top: Fishtail 01; Bottom: Fishtail 05 (R), Fishtail 09 (L).

CONCLUSIONS

Based on the numerical results of twelve fishtail foils, the following conclusions are conducted:

(1) From the validation by using NACA 0012 Airfoil, the CFD results of the present study are reliable.

(2) At high Reynolds number, the lift and drag of foils are not significantly influenced by Reynolds number.

(3) Fishtails of rudder increase the lift force and the larger trailing edge produces higher lift force. The high lift is generated by the high pressure created at the concave of face side of the fishtail.

(4) Fishtails increase drag force and the larger trailing edge causes higher drag. Dead waters generated at the concaves of the fishtail reduce the drag at zero or small angle of attack.

(5) From the high lift and low drag point of view: Fishtail with small trailing edge and medium maximum thickness gives the better hydrodynamic than others.

REFERENCES

Douvi, CE, Tsavalos, LA and Margaris, PD (2012). Evaluation of the Turbulence Models for the Simulation of the Flow over a National Advisory Committee for Aeronautics (NACA) 0012 airfoil. *Journal of Mechanical Engineering Research,* Vol. 4(3), pp. 100-111.

Gregory, N and O'Reilly, CL (1970). "Low-Speed Aerodynamic Characteristics of NACA 0012 Aerofoil Sections, including the Effects of Upper-Surface Roughness Simulation Hoar Frost," NASA R&M 3726.

Hasegawa, K, Kang, DH, Nishikouri, H, Yamada, H, Yamaguchi, M, Tanaka, Y and Arii, T (2004). Manoeuvrability Prediction of Pure Car Carrier Installed with Schilling Rudder. *Proc. of the 2nd Asia-Pacific Workshop on Marine Hydrodynamics*, APHydro 2004, pp 293-299.

Hasegawa, K, Nagarijian, V, and Kang, DH (2006). Performance evaluation of Schilling rudder and mariner rudder for pure car carriers (PCC) under wind condition. *International Conference on Marine Simulation and Ship Manoeuvrability*, MARSIM2006, pp.M-5-1 - M-5-10.

Hoerner, SF and Borst, HV (1975). Fluid-Dynamic-Lift.

Kimura, Y, Yamasita, M and Yuda, N (2008). Study on Hydrodynamic Forces Acting on Rudder of Fish-Shape Section with End Plates-II: The Influence of Tail Length and Trailing Edge Thickness of the Rudder. *Japan Institute of Navigation Proceedings* (119), pp 119-127.

Ladson, CL (1988). "Effects of Independent Variation of Mach and Reynolds Numbers on the Low-Speed Aerodynamic Characteristics of the NACA 0012 Airfoil Section," NASA TM 4074.

Molland, AF and Turnock, SR (2007). Marine Rudder and Control Surface.

Nagarajan, V, Kang, DH, Hasegawa, K and Nabeshima, K (2008). Comparison of the mariner Schilling rudder and the mariner rudder for VLCCs in strong winds. *Journal of marine science and technology*, 13(1), pp 24-39.

NASA LaRC. Turbulence Modeling Resource-2D NACA 0012 Airfoil Validation Case.

Yuda, N, Yamashita, M, Kurimoto, H and Yamashita, T (2007). A Consideration on Hydrodynamic Forces Acting on the Rudder of Fish-Shape Section with End Plates -Based on Experiments Using Rudder Models. *Yuge National College of Maritime Technology Bulletin*, 29, pp 7-12.

Yuda, N, Yamasita, T, Iwasaki, K, Kihara, Y, Itou, Y and Mukai, T (2010a). A Study on Hydrodynamic Forces Acting on the Rudder of Fish-Shape Section with End Plates - Based on Experiments Using Rudder Models *Yuge National College of Maritime Technology Bulletin*, 32, pp 13-18.

Yuda, N, Yamasita, T, Iwasaki, K, Kihara, Y, Itou, Y and Mukai, T (2010b). A Study on Hydrodynamic Forces Acting on the Rudder of Fish-Shape Section with End Plates in Propeller Slipstream. *Yuge National College of Maritime Technology Bulletin*, 32, pp 13-18.